Monte Carlo simulations on mesophase formation using dipolar Gay-Berne model

Katsuhiko Satoh[a]; Shigeru Mita[a]; Shoichi Kondo[a]

[a] Department of Chemistry, Faculty of Science, Science University of Tokyo, Tokyo, Japan

PLEASE SCROLL DOWN FOR ARTICLE

Monte Carlo simulations on mesophase formation using dipolar Gay–Berne model

by KATSUHIKO SATOH*, SHIGERU MITA and SHOICHI KONDO

Department of Chemistry, Faculty of Science, Science University of Tokyo,
1-3 Kagurazaka, Shinjuku-ku, Tokyo 162, Japan

We report the results of a Monte Carlo simulation of polar particles interacting via the Gay–Berne potential combining dipole–dipole interactions. Simulations were carried out on a system of 256 particles with either a zero dipole moment or longitudinal dipole moment located at the centre of the molecule. The system was found to spontaneously form nematic, smectic and crystal phases from an isotropic phase with a random configuration as temperature was decreased, irrespective of values of the dipole moment. The results do not give any indication of a net polarization even in the system with a strong dipole moment ($\mu^* = 2\cdot00$). The transition temperature from the isotropic to nematic phase is not sensitive to the value of the dipole moment within the limits of statistical error, while the transition from the nematic to smectic phase depends on the strength of dipole moment. At lower temperatures forming the smectic or the crystal phase, the translational order along the director increases with increasing dipole moment. The dipolar interactions contribute to the long range ordering.

1. Introduction

Monte Carlo (MC) and molecular dynamics (MD) simulations are a powerful tool for analysing the molecular structures and motions in liquid crystal phases.

MC simulations by Frenkel and co-workers [1–5] found that the nematic and smectic phases appear in the system of the freely rotating hard spherocylinders with $L/D = 5$. In the case of a hard ellipsoid with $L/D = 3$ the nematic phase appeared for a small density range (0·329–0·365), but a stable density wave order could not be formed irrespective of L/D.

For a system composed of prolate ellipsoidal particles interacting with each other via the Gay–Berne (GB) potential consisting of soft repulsive and attractive forces, the molecular dynamics simulations showed that the isotropic, nematic, smectic B and crystalline phases can be formed in the system along different isotherms [6, 7]. In addition, as shown by Emerson et al., the oblate GB molecules could form a columnar phase [8].

The dipolar effect on the structure and thermodynamic properties of dipolar hard ellipsoids and dipolar hard spherocylinders was recently examined by using Monte Carlo simulations on the isotropic and/or smectic phases at constant temperatures by Levesque et al. [9, 10].

Wei and Patey showed that strongly interacting dipolar hard spheres can form a ferroelectric nematic

phase by MD simulation [11]. In the case of the system consisting of hard ellipsoids $(L/D = 3)$ with a central longitudinal dipole moment, the nematic phase did not appear except for a narrow density range (0·32–0·36) in which the crystalline phase formed [10].

Thus, for the hard particles with $L/D = 3$, the attractive force turned out to be crucial for the formation of the nematic phase. Further, the role of the dipole–dipole interaction for stabilizing mesophases or for transition behaviour is not yet clear despite a great number of polar molecules in conventional liquid crystals. We have investigated the effect of the dipolar interaction on liquid crystal formation for particles interacting via a uniaxial GB potential with variation in temperature.

The long range interactions between dipolar molecules can usually be handled by two different approaches, namely the Ewald summation technique and the Reaction Field (RF) method [12, 13]. The first of these approaches is based on the assumption of the periodicity of the same sample and it yields results for a model with an infinite-range potential. Its main disadvantage lies in the fact that it is very time consuming. On the other hand, the RF method uses a truncated potential in which the effects of the long range dipolar interactions are corrected by surrounding the truncation sphere with a polarizable dielectric continuum.

In this paper the long range dipolar interaction has been calculated by the RF method because of easy programming and to enable a more immediate comparison between the simulation and theoretical results.

*Author for correspondence.

The potential model and computational detail are described in §2. Numerical results and discussion are presented in §3. In §4 our conclusions are given.

2. Potential model and method

The total pair potential used can be expressed in the form

$$U_{\text{Total}} = U_{\text{GB}} + U_{\text{Dipole}} \tag{1}$$

where U_{GB} is the GB potential [14],

$$U_{\text{GB}}(\hat{\mathbf{u}}_i, \hat{\mathbf{u}}_j, \mathbf{r}) = 4\varepsilon(\hat{\mathbf{u}}_i, \hat{\mathbf{u}}_j, \hat{\mathbf{r}}) \times \left[\left\{ \frac{\sigma_0}{r - \sigma(\hat{\mathbf{u}}_i, \hat{\mathbf{u}}_j, \hat{\mathbf{r}}) + \sigma_0} \right\}^{12} \right.$$
$$\left. - \left\{ \frac{\sigma_0}{r - \sigma(\hat{\mathbf{u}}_i, \hat{\mathbf{u}}_j, \hat{\mathbf{r}}) + \sigma_0} \right\}^{6} \right] \tag{2}$$

where $\hat{\mathbf{u}}_i$ stands for the axial vector of particle i, and $\hat{\mathbf{r}}$ is the unit vector of interparticle vector $\mathbf{r} = \mathbf{r}_i - \mathbf{r}_j$, and $r = |\mathbf{r}_i - \mathbf{r}_j|$ is the particle separation in which $\mathbf{r}_i$ and $\mathbf{r}_j$ are the positional vectors of centres of particles i and j, respectively. The potential parameters are as follows; σ_0 is a constant, $\varepsilon(\hat{\mathbf{u}}_i, \hat{\mathbf{u}}_j, \hat{\mathbf{r}})$ is the potential well depth and $\sigma(\hat{\mathbf{u}}_i, \hat{\mathbf{u}}_j, \hat{\mathbf{r}})$ is the interparticle separation given in the Berne–Pechukas–Kushick function [15]. We used the parameters for the GB potential, axial ratio $\sigma_e/\sigma_s = 3\cdot0$, and well depth ratio $\varepsilon_e/\varepsilon_s = 0\cdot2$ and exponent parameters (μ, ν) were used, as introduced by Luckhurst *et al.* [7].

U_{Dipole} is dipole–dipole interaction,

$$U_{\text{Dipole}} = \frac{(\mu_i \cdot \mu_j)r^2 - 3(\mu_i \cdot \mathbf{r})(\mu_j \cdot \mathbf{r})}{r^5} \tag{3}$$

where μ is longitudinal dipole moment located at the centre of particle.

We used a tetragonal cell as the simulation box with the usual periodic boundary conditions in order to accommodate an appropriate number of the smectic layers. Monte Carlo calculations with 256 particles were done in the standard sampling scheme introduced by Metropolis *et al.* [16]. A series of simulations was performed in the range of 0·60 to 3·50 for reduced temperatures T^* ($\equiv kT/\varepsilon_0$) and of 0·00, 1·00, 1·50 and 2·00 for reduced dipole moments μ^* ($\equiv \mu/(\sigma_0^3\varepsilon_0)^{1/2}$) at fixed reduced number density ρ^* ($\equiv N\sigma_0^3/V$) = 0·30.

In all calculations the cut-off radius beyond which the short range interaction potential was set equal to zero was the half the shorter cell length ($L_{\text{min}}/2 \approx 4\cdot2\sigma_s$). The long range dipolar interaction is treated by the RF method as described previously. The additional term of the Reaction Field is defined as [17]

$$U_{ij}^{\text{RF}} = -\frac{2(\varepsilon' - 1)}{2\varepsilon' + 1} \frac{\mu_i \cdot \mu_j}{r_c^3}, \quad r_{ij} < r_c,$$
$$= 0, \quad r_{ij} \geqslant r_c \tag{4}$$

where r_c is the cut-off distance and ε' the dielectric constant of the continuum.

In order to analyse the orientational structure, the first and second orientational order parameters $\langle P_1 \rangle$, $\langle P_2 \rangle$ and the dipole–dipole correlation function $h(r)$ were calculated as follows.

$$P_1 = \frac{1}{N} \left| \sum_{i=1}^{N} \hat{\mathbf{u}}_i \cdot \hat{\mathbf{d}} \right| \tag{5}$$

where $\hat{\mathbf{d}}$ is the director corresponding to the eigenvector Q as below. The order parameter $\langle P_2 \rangle$ is defined as the average of the largest eigenvalue of the tensor [13, 18],

$$Q_{\alpha\beta} = \frac{1}{N} \sum_{i=1}^{N} \frac{1}{2}(3\hat{\mathbf{u}}_{i\alpha}\hat{\mathbf{u}}_{i\beta} - \delta_{\alpha\beta}) \tag{6}$$

where $\hat{\mathbf{u}}_{i\alpha}$ is the α-component of the unit vector along the symmetry axis of particle i, and the director corresponds to the eigenvector. The dipole–dipole correlation function $h(r)$ is defined as

$$h(r) = 3\langle \cos\theta_{ij}(r) \rangle \tag{7}$$

where θ_{ij} is the angle between the axis of two particles separated by r.

In the series of calculations, initial configurations have been set in an isotropic state, being randomly oriented particles. We have examined the results of phase formation spontaneously obtained by cooling.

At each temperature, the system was equilibrated for $5\cdot0 \times 10^5$ to $3\cdot0 \times 10^6$ MC steps and then an additional $1\cdot0 \times 10^5$ MC steps were generated. Successive calculations on reducing temperature were started from the preceding final configurations.

3. Results and discussion
3.1. *Orientational order*

The temperature dependence of the first and the second orientational order parameter $\langle P_1 \rangle$, $\langle P_2 \rangle$ for the systems with various dipole moments is shown in figure 1. It can be seen that $\langle P_2 \rangle$ changes sharply at steady temperatures $T^* = 2\cdot20$–$2\cdot30$, regardless of the magnitude of dipole moment. In contrast to this variation, the change of $\langle P_2 \rangle$ at $T^* = 1\cdot20$–$1\cdot60$ shifted slightly to higher temperatures proportional to the strength of dipole moment. The results for the non-polar system are in accord with those obtained using a cubic cell by Luckhurst *et al.* [7]. In all temperature ranges, the values of $\langle P_1 \rangle$ were almost zero and no net polarization appeared for all systems. These systems have no net polarization even when the $\langle P_2 \rangle$ value is not zero. Therefore the dipolar GB molecules did not show any ferroelectric liquid crystal phases. This result agrees with the findings of MC simulations for dipolar hard spherocylinders obtained by Levesque *et al.* [9].

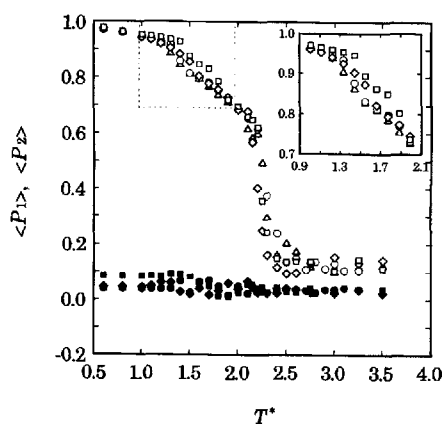In figure 2 the variations of the averaged potential

Figure 1. Temperature dependence of the first- and the second-rank orientational order parameters: $\langle P_1 \rangle$ filled and $\langle P_2 \rangle$ open symbols; triangles, circles, diamonds and squares for $\mu^* = 0.00$, 1.00, 1.50 and 2.00, respectively.
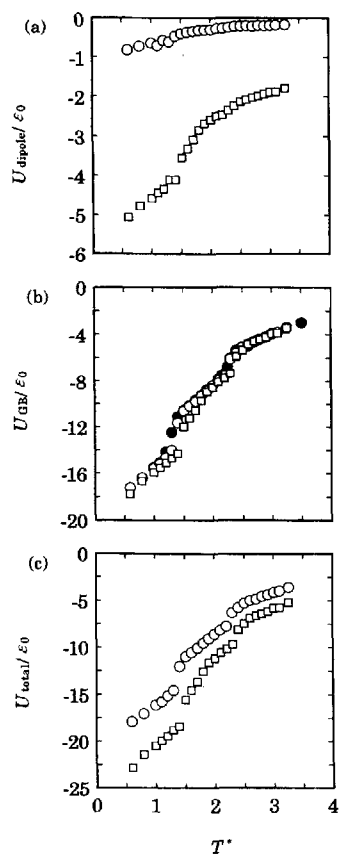

Figure 2. (a) The average dipole–dipole interaction energy, (b) GB energy and (c) total energy as a function of temperature for $\mu^* = 0.00$ (●), 1.00 (○) and 2.00 (□).

energy, GB energy and dipole–dipole interaction energy with temperature are shown. On reducing temperature, two discontinuities corresponding to phase transitions can be seen at higher and lower temperatures. One of

them is noted by a small jump in the energy at $T^* = 2.20$–2.30. From the total energy for $\mu^* = 2.00$, a small shift seems to be apparent. It is difficult to conclusively state whether the transition temperature depends on the strength of dipole moment or not, as a result of statistical fluctuations in the order parameter. The other phase transition is also indicated by energy jumps in $T^* = 1.20$–1.70. The transition temperature apparently shifted toward higher temperatures with increasing strength of the dipole moment.

Consequently, two transitions were found in all systems. The higher temperature transition was substantially independent of μ^* values, but the lower temperature transition was sensitive to the strength of the dipole moment.

3.2. Positional order

In figure 3, we present snapshots of instantaneous configuration for $\mu^* = 0.00$ and 2.00 in the vicinity of the higher transition temperature. Phases with a positional order are expected to appear on reducing temperature. In both systems positional ordered phases were still not formed in spite of the highly orientational ordered state which began to appear around this temperature.

In order to compare positional order formed in a non-polar system with that in a polar one, we calculated
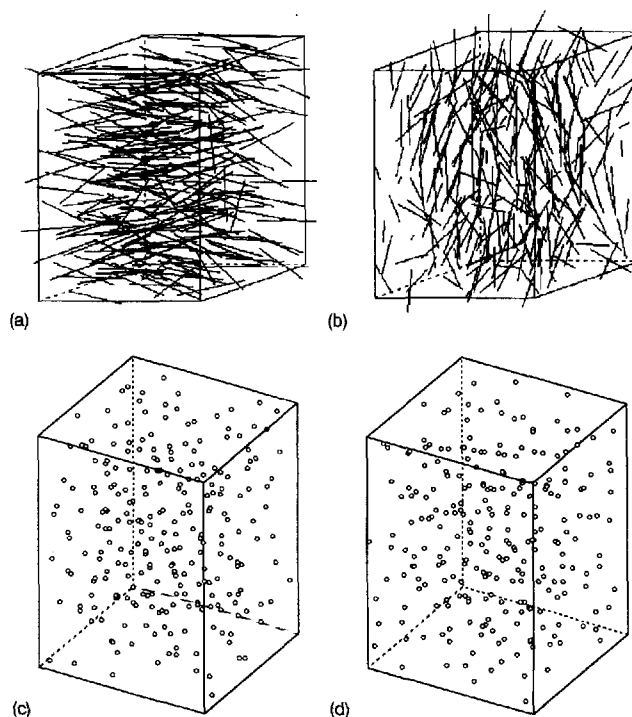

Figure 3. The snapshots of instantaneous configurations at $T^* = 2.00$; (a), (c): for $\mu^* = 0.00$ (b), (d): for $\mu^* = 2.00$, (c) and (d): centres of mass only are displayed.

the transverse and longitudinal positional pair correlation functions, $g_\perp(r_\perp^*)$ and $g_\parallel(r_\parallel^*)$, where $r_\perp^*$ and $r_\parallel^*$ are the separation between a pair of particles when their centre-of-mass coordinates are projected perpendicularly and parallel to the director. These functions at $T^* = 2\cdot00$ are shown in figure 4. The longitudinal functions, $g_\parallel(r_\parallel^*)$ show no correlation in both systems. The correlation in the transverse $g_\perp(r_\perp^*)$ shows that the molecules have a short range order such as an isotropic liquid (I). The molecules have the orientational order shown in figures 1 and 3, so we identify the structure to be that of a nematic phase (N).

In a theoretical study of fluids of prolate particles, a dipolar force was found to have a significant effect upon the isotropic–nematic transition which occurred even at lower densities as the dipole moment was increased [19]. MC results for the system of hard ellipsoids (elongation: 3) showed that the nematic phase was only stable in a very narrow density domain close to that of the solid phase, and that the phase behaviour was not modified by interactions between the central dipolar ellipsoids [10]. In contrast with the above cases, our results showed that a stable nematic phase was found, and the N–I transition temperature was not sensitive to the dipole moment.

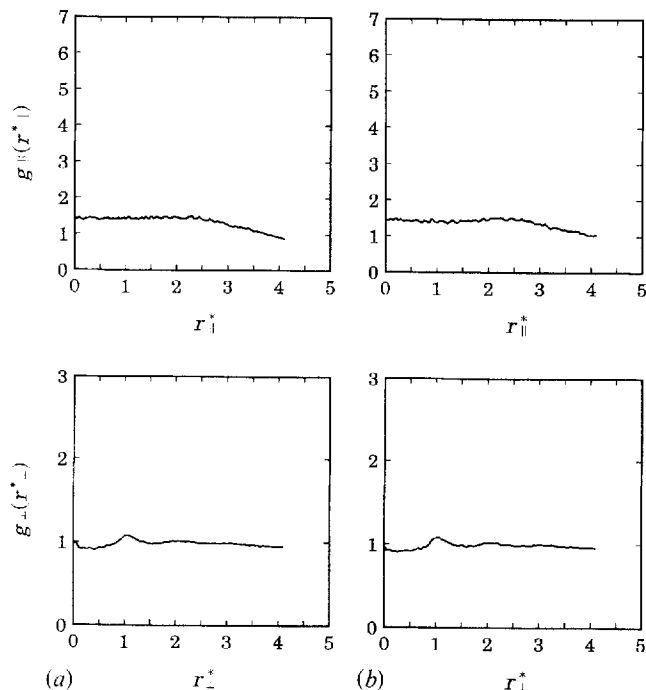The snapshots of instantaneous configurations at $T^* = 1\cdot60$ for the non-polar and strong polar systems ($\mu^* = 2\cdot00$) are shown in figure 5. As shown in (b) and (d), not only an orientationally ordered state was formed, but a positional ordered one also formed for the polar system. No significant tilt of the director relative to the layer normal was indicated in the snapshots, thus the phase can be identified as a smectic A phase. On the other hand, the positional order was still not formed in the case of the non-polar system.

The longitudinal pair correlation functions $g_\parallel(r_\parallel^*)$ in the vicinity of the nematic–smectic (S) transition temperature for all systems studied are shown in figure 6. In the strongest polar system ($\mu^* = 2\cdot00$) an intense correlation peak at r^* of $c.\ 2\cdot6$ indicated the formation of a kind of layer structure at a temperature of $1\cdot70$, but it exhibited only weak peak at T^* of $1\cdot80$. There was a tendency for the layer spacing to become longer, thus the dipole interaction tends to enhance the correlation of molecular position within a layer. In the non-polar system a change was found to have occurred at a temperature between $1\cdot30$ and $1\cdot40$. In $g_\parallel(r_\parallel^*)$ for all systems correlation peaks indicate a considerable interpenetration of molecules from one layer into the next because the position of the peak is smaller than $3\cdot0$ of the particle elongation. Therefore, the smectic phase was formed through the nematic phase from the isotropic phase for decreasing temperature regardless of the strength of dipole moment, and the N→S transition

Figure 4. The longitudinal and transverse pair correlation functions, $g_\parallel(r_\parallel^*)$, $g_\perp(r_\perp^*)$ at $T^* = 2\cdot00$ for (a) $\mu^* = 0\cdot00$ and (b) $2\cdot00$.
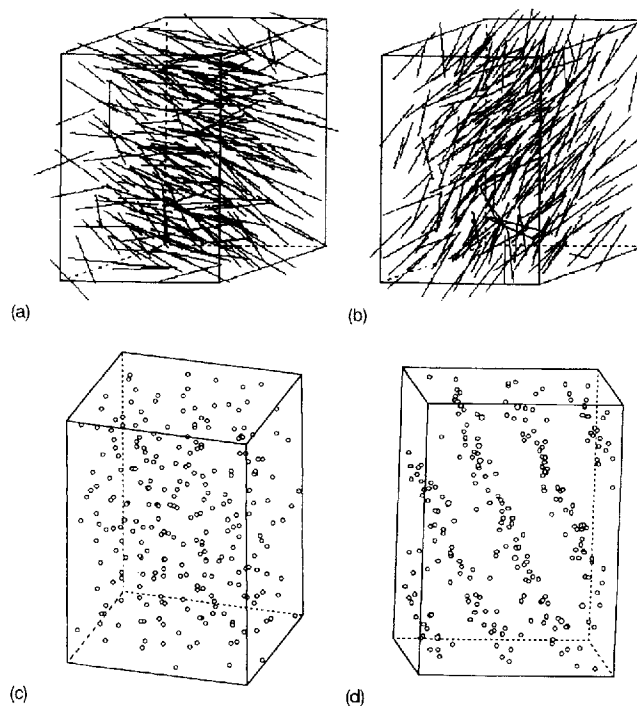

Figure 5. The snapshots of instantaneous configurations at $T^* = 1\cdot60$; (a), (c): for $\mu^* = 0\cdot00$ (b), (d): for $\mu^* = 2\cdot00$, (c) and (d): centres of mass only are displayed.
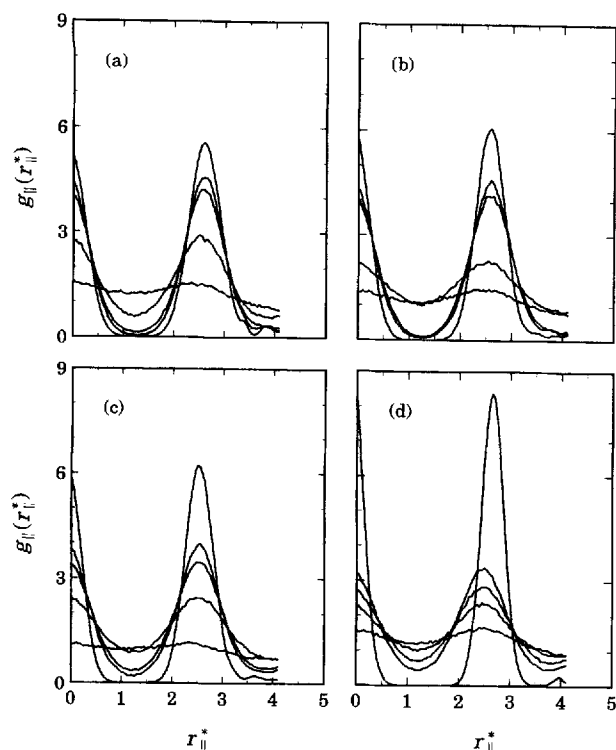
Figure 6. The longitudinal pair correlation functions, $g_\parallel(r_\parallel^*)$ for (a) $\mu^* = 0.00$, (b) 1.00, (c) 1.50 and (d) 2.00. From the top peak to bottom, the temperatures considered are (a) 0.60, 1.10, 1.20, 1.30, 1.40, (b) 0.60, 1.20, 1.30, 1.40, 1.50, (c) 0.60, 1.30, 1.40, 1.50, 1.60, (d) 0.60, 1.50, 1.60, 1.70, 1.80.

Figure 7. The transverse pair correlation functions, $g_\perp(r_\perp^*)$ for (a) $\mu^* = 0.00$ and (b) 2.00. From top to bottom, the temperatures considered are 0.60, 1.10, 1.20, 1.30, 1.40, 1.70 and 1.80.

temperature was influenced by the interactions between longitudinal dipole moments. The N → S transition temperatures are estimated to be $T^* = 1.30$, 1.40, 1.50, 1.70 for $\mu^* = 0.00$, 1.00, 1.50, 2.00 from the inspection of the correlation functions with temperature in figures 1 and 6, respectively.

In order to clear the transition of smectic to crystalline phase, the transverse pair correlation functions $g_\perp(r_\perp^*)$ at various temperatures for the strong polar and non-polar systems are shown in figure 7. In the polar system at a temperature of 1.40 the transverse pair correlations do not have strong peaks which suggest a long range positional order perpendicular to the director, although the layer structure had already formed below a temperature of 1.70 as shown in figure 6. Hence it is clear that this phase is a smectic phase at this temperature. The transition temperature from the smectic to crystal phase depended a little on the dipole moment, although the dependency was not clear in comparison with the nematic to smectic transition. The dipolar interaction between particles contributes to a spread in the temperature range of the smectic phase. The smectic to crystal phase transition temperature was found to be 1.20–1.30
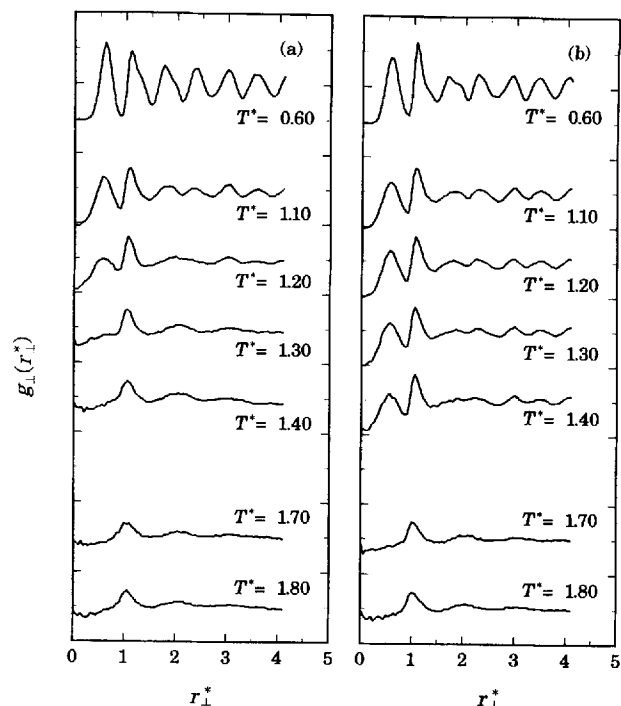
for the strong polar system ($\mu^* = 2.00$) and 1.10 for the non-polar system.

The first peak ($r^* = c. 0.6$) arising from correlation with particles in the other layers was the strongest peak at $T^* = 0.60$ in the non-polar system, and the correlation function was found to decrease with distance. On the contrary in the smectic phase of the polar system the strongest peak ($r^* = c. 1.1$) corresponds to the correlation between nearest neighbour particles in a layer, and the same relation is also obtained in the crystal phase (for example, $T^* = 0.60$). Thus, this correlation peak was stronger than the first peak from particles out of the layer in the smectic and crystal phases. It is suggested that the dipolar interaction plays a role for ordering molecular position within a layer and for stabilizing the layer structure.

Conclusively, the N–I transition occurred at almost the same temperature $T^* = 2.20$–2.30 for all systems studied, but the S–N transition temperature slightly shifted to higher temperatures as the strength of dipole moment increased.

To show the layer formation more clearly, projections of the centre of masses on a plane parallel to the director for the systems with $\mu^* = 0.00$ and 2.00 are shown in figure 8. Although peak heights depending on the layer structure formed from the initial isotropic configuration
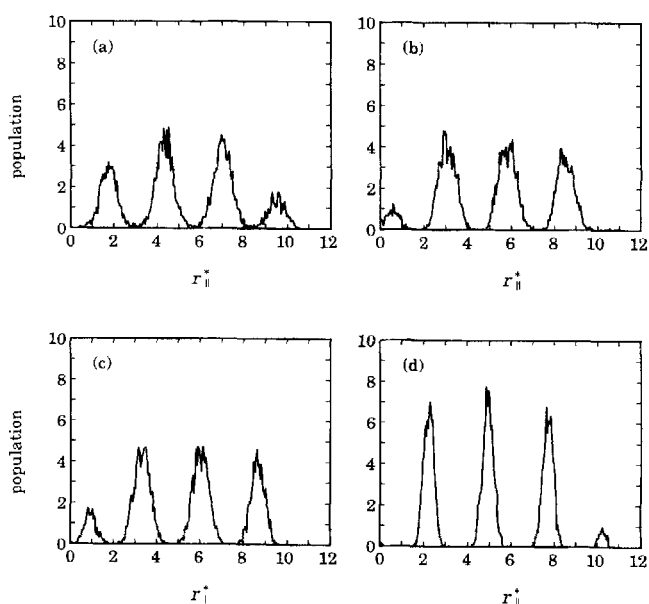
Figure 8. The distributions for position of centre of mass along the director; (a) $T^* = 1\cdot20$, $\mu^* = 0\cdot00$, (b) $T^* = 1\cdot20$, $\mu^* = 2\cdot00$, (c) $T^* = 0\cdot60$, $\mu^* = 0\cdot00$, (d) $T^* = 0\cdot60$, $\mu^* = 2\cdot00$.

are different from each other, the sharpness of peak is a measure of the translational order in the direction of the director. The four layers in the smectic phase formed spontaneously through the nematic phase from the isotropic phase on cooling are illustrated for both systems. While the sharpness of distribution was independent of the strength of the dipole moment at $T^* = 1\cdot20$, the sharpness was appreciably dependent on it at $T^* = 0\cdot60$. The spacing between adjacent layers was almost the same for both cases, but the distribution for $\mu^* = 2\cdot00$ appeared to be much sharper than that for $\mu^* = 0\cdot00$.

Levesque *et al.* [9] studied systems consisting of hard spherocylinders of a length-to-breadth ratio of 6 with the dipole moment located at various distances from the centre of the particles. In the case of a central dipole moment, the centre of mass density modulation of the S_A phase is indistinguishable, within statistical error, from the corresponding function obtained for a system of non-polar molecules. In the dipolar GB model consisting of soft repulsive and attractive forces, we have also obtained the similar result at $T^* = 1\cdot20$. On the other hand, the centre of mass density modulation for the polar system was apparently found to be sharper than that of the non-polar system for lower temperatures ($T^* = 0\cdot60$). Therefore the dipolar interaction and anisotropic attractive force play a significant role for stabilizing the layer structure.

3.3. *Microstructure*

There should be a tendency of the molecules to have an antiparallel arrangement in the short range since

such an arrangement is energetically favourable if the dipole moments are close to each other. We intend to investigate this possibility by calculating a dipole–dipole correlation function as defined in equation (7). It can easily be derived that negative values of the function are associated with dipoles aligned antiparallel. As can be seen in figure 9, the antiparallel arrangement was much larger than the parallel arrangement at the first nearest neighbour; on the other hand, the parallel arrangement was the preferential arrangement of dipole pairs at the second nearest neighbour. Such a tendency is pronounced for molecules with decreasing temperature. Although there are local regions of antiparallel association of dipole moments, the system is not globally ferroelectric. It is noticed that the dipole moment contributes to the formation of long range order since the correlation appears for the molecular pair even in the third neighbour. It is also apparent from figure 9 that the maximum position of the first peak for antiparallel pairs is slightly smaller than that for parallel pairs.

In order to better establish a microstructure and its temperature dependence, we have calculated populations for parallel or antiparallel pairs with the intermolecular distance. Figure 10 shows the population of dipolar pair alignment at $T^* = 1\cdot20$ (smectic phase) and $T^* = 0\cdot60$ (crystal phase). In the case of stronger dipole moments, it is seen that antiparallel pairs in the nearest neighbour outnumber the parallel pairs in the crystal and smectic phases.
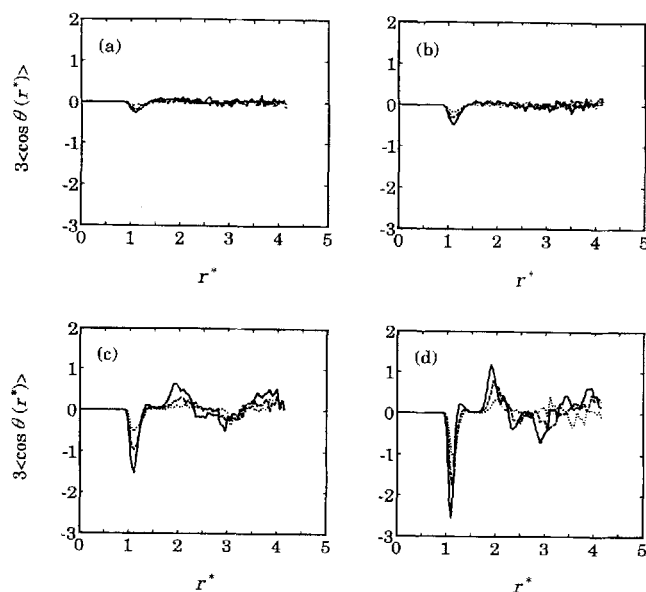

Figure 9. The dipole–dipole correlation functions $h(r^*) = 3\langle\cos\theta_{ij}(r^*)\rangle$ for $\mu^* = 0\cdot00$ (dotted line), $1\cdot50$ (broken line) and $2\cdot00$ (solid line) at (a) $T^* = 2\cdot50$, (b) $T^* = 2\cdot00$, (c) $T^* = 1\cdot20$ and (d) $T^* = 0\cdot60$.
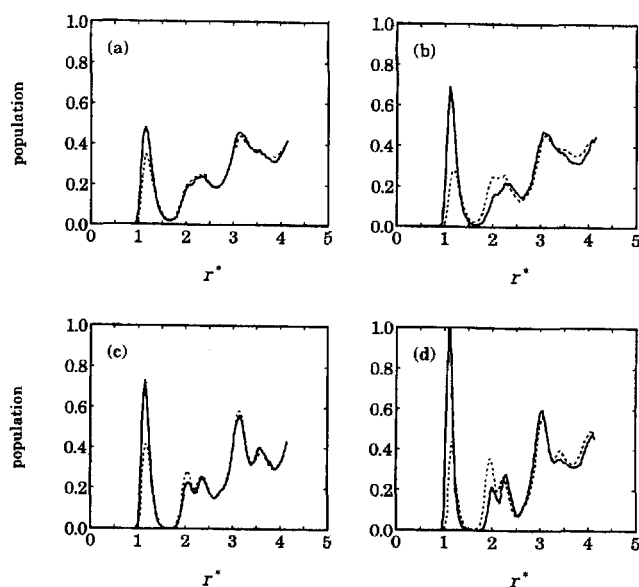
Figure 10. The populations of parallel ($\cdots$) and antiparallel
(——) pairs as a function of separation r^*; (a) $T^* = 1.20$,
$\mu^* = 0.00$, (b) $T^* = 1.20$, $\mu^* = 2.00$, (c) $T^* = 0.60$, $\mu^* = 0.00$, (d) $T^* = 0.60$, $\mu^* = 2.00$.

4. Conclusions

We carried out a preliminary study of the effect of the dipole moment on the mesophase formation by a Monte Carlo simulation using a GB potential. The system of particles interacting via the potential is found to exhibit a series of phases as the temperature is lowered from the isotropic phase. These phases have been identified by the order parameters and the correlation functions. The N–I transition is scarcely affected by the longitudinal dipole moment, but the N–S transition does depend on it. The smectic temperature range in the strong polar system was somewhat wider than that in the non-polar system.

On the layer structure formed, the density modulation for the system of strongly polar molecules is much sharper than that for the non-polar system at lower temperatures.

In the smectic and crystal phases, correlations of $g_{\parallel}(r_{\parallel}^*)$ and $g_{\perp}(r_{\perp}^*)$ in a layer were more evident as compared to those out of the layer for the polar system. It suggests that the dipole moment makes particles attractive for layer formation and brings about the stabilization of layer structures.

We confirm that the population of antiparallel arrangements is much larger than that of parallel pairing

in the first nearest neighbour, while the tendency reverses in the second nearest neighbour.

References

[1] STROOBANTS, A. W., LEKKERKERKER, H. N., and FRENKEL, D., 1986, *Phys. Rev. lett.*, **57**, 1452; STROOBANTS, A. W., LEKKERKERKER, H. N., and FRENKEL, D., 1987, *Phys. Rev. A*, **36**, 2929.

[2] FRENKEL, D., LEKKERKERKER, H. N. W., and STROOBANTS, A., 1988, *Nature (London)*, **332**, 822.

[3] VEERMAN, J. A. C., and FRENKEL, D., 1991, *Phys. Rev. A*, **43**, 4334.

[4] FRENKEL, D., MULDER, B. M., AND MCTAGUE, J. P., 1985, *Mol. Cryst. liq. Cryst.*, **123**, 119.

[5] FRENKEL, D., and MULDER, B. M., 1985, *Mol. Phys.*, **55**, 1171.

[6] DE MIGUEL, E., RULL, L. F., CHALAM, M. K., and GUBBINS, K. E., 1990, *Mol. Phys.*, **71**, 1223; 1991, *Ibid.*, **74**, 405; DE MIGUEL, E., RULL, L. F., CHALAM, M. K., GUBBINS, K. E., and SWOL, F. V., 1991, *Mol. Phys.*, **72**, 593; DE MIGUEL, E., RULL, L. F., and GUBBINS, K. E., 1992, *Phys. Rev. A*, **45**, 3813.

[7] LUCKHURST, G. R., STEPHENS, R. A., and PHIPPEN, R. W., 1990, *Liq. Cryst.*, **8**, 451; ADAMS, D. J., LUCKHURST, G. R., and PHIPPEN, R. W., 1987, *Mol. Phys.*, **61**, 1575.

[8] EMERSON, A. P. J., LUCKHURST, G. R., and WHATLING, S. G., 1994, *Mol. Phys.*, **82**, 113.

[9] LEVESQUE, D., WEIS, J. J., and ZARRAGOICOECHEA, G. J., 1993, *Phys. Rev. E*, **47**, 496; WEIS, J. J., LEVESQUE, D., and ZARRAGOICOECHEA, G. J., 1992, *Phys. Rev. Lett.*, **69**, 913.

[10] ZARRAGOICOECHEA, G. J., LEVESQUE, D., and WEIS, J. J., 1992, *Mol. Phys.*, **75**, 989; 1991, *Ibid.*, **74**, 629.

[11] WEI, D., and PATEY, G. N., 1992, *Phys. Rev. Lett*, **68**, 2043; WEI, D., and PATEY, G. N., 1992, *Phys. Rev. A*, **46**, 7783.

[12] GRAY, C. G., SAINGER, Y. S., JOSLIN, C. G., CUMMINGS, P. T., and GOLDMAN, S., 1986, *J. chem. Phys.*, **85**, 1502.

[13] ALLEN, M. P., and TILDESLEY, D. J., 1989, *Computer Simulation of Liquids* (Oxford: Clarendon) and references therein.

[14] GAY, J. G., and BERNE, B. J., 1981, *J. chem. Phys.*, **74**, 3316.

[15] BERNE, B. J., and PECHUKAS, P., 1972, *J. chem. Phys.*, **56**, 4213; KUSHICK, J., and BERNE, B. J., 1976, *J. chem. Phys.*, **64**, 1362.

[16] METROPOLIS, N., ROSENBLUTH, A. W., ROSENBLUTH, M. N., TELLER, A. H., and TELLER, E., 1953, *J. chem. Phys.*, **21**, 1087.

[17] NEUMANN, M., 1983, *Mol. Phys.*, **50**, 841.

[18] ZANNONI, C., 1979, *The Molecular Physics of Liquid Crystals*, edited by G. R. Luckhurst and G. W. Gray (London: Academic Press), Chap. 3.

[19] PERERA, A., and PATEY, G. N., 1989, *J. chem. Phys.*, **91**, 3045.